



HAL
open science

Temperature is a key factor in *Micromonas*-virus interactions

David Demory, Laure Arsenieff, Nathalie Simon, Christophe Six, Fabienne Rigaut-Jalabert, Dominique Marie, Pei Ge, Estelle Bigeard, Stéphan Jacquet, Antoine Sciandra, et al.

► To cite this version:

David Demory, Laure Arsenieff, Nathalie Simon, Christophe Six, Fabienne Rigaut-Jalabert, et al.. Temperature is a key factor in *Micromonas*-virus interactions. *The International Society of Microbiological Ecology Journal*, 2017, 11 (3), pp.601-612. 10.1038/ismej.2016.160 . hal-01464528

HAL Id: hal-01464528

<https://hal.sorbonne-universite.fr/hal-01464528>

Submitted on 10 Feb 2017

HAL is a multi-disciplinary open access archive for the deposit and dissemination of scientific research documents, whether they are published or not. The documents may come from teaching and research institutions in France or abroad, or from public or private research centers.

L'archive ouverte pluridisciplinaire **HAL**, est destinée au dépôt et à la diffusion de documents scientifiques de niveau recherche, publiés ou non, émanant des établissements d'enseignement et de recherche français ou étrangers, des laboratoires publics ou privés.

1 **Temperature is a key factor in *Micromonas* - virus interactions**

2 D. Demory ^{a,b*}, L. Arsenieff ^c, N. Simon ^c, C. Six ^c, F. Rigaut-Jalabert ^d, D. Marie ^c,
3 P. Gei ^c, E. Bigeard ^c, S. Jacquet ^e, A. Sciandra ^a, O. Bernard ^b, S. Rabouille ^a and A-
4 C. Baudoux ^c

5

6 ^a Sorbonne Universités, UPMC Univ Paris 06, CNRS, UMR 7093, LOV, Observatoire
7 océanologique, F-06230, Villefranche/mer, France

8 ^b BIOCORE-INRIA, BP93, 06902 Sophia-Antipolis Cedex, France

9 ^c Sorbonne Universités, UPMC Univ Pierre et Marie Curie (Paris 06), CNRS,
10 Adaptation et Diversité en Milieu Marin UMR7144, Station Biologique de Roscoff,
11 29680 Roscoff, France

12 ^d Sorbonne Universités, UPMC Univ Pierre et Marie Curie (Paris 06), CNRS,
13 Fédération de Recherche FR2424, Station Biologique de Roscoff, 29680 Roscoff,
14 France

15 ^e INRA, UMR CARRTEL, 75 Avenue de Corzent, 74203 Thonon-les-Bains Cedex,
16 France

17

18

19 * Corresponding author: david.demory@obs-vlfr.fr

20

21

22 **Abstract**

23

24 The genus *Micromonas* comprises phytoplankton that show among the widest
25 latitudinal distributions on Earth and members of this genus are recurrently infected
26 by prasinoviruses in contrasted thermal ecosystems. In this study, we assessed how
27 temperature influences the interplay between the main genetic clades of this
28 prominent microalga and their viruses. The growth of 3 *Micromonas* strains (Mic-A,
29 Mic-B, Mic-C) and the stability of their respective lytic viruses (MicV-A, MicV-B,
30 MicV-C) were measured over a thermal range of 4 to 32.5 °C. Similar growth
31 temperature optima (T_{opt}) were predicted for all three hosts but Mic-B exhibited a
32 broader thermal tolerance than Mic-A and Mic-C, suggesting distinct
33 thermoacclimation strategies. Similarly, the MicV-C virus displayed a remarkable
34 thermal stability compared to MicV-A and MicV-B. Despite these divergences,
35 infection dynamics showed that temperatures below T_{opt} lengthened lytic cycle
36 kinetics and reduced viral yield and, notably, that infection at temperatures above T_{opt}
37 did not usually result in cell lysis. Two mechanisms operated depending on the
38 temperature and the biological system. Hosts either prevented the production of viral
39 progeny or they maintained their ability to produce virions with no apparent cell lysis,
40 pointing to a possible switch in viral life strategy. Hence, temperature changes
41 critically affect the outcome of *Micromonas* infection and have implications for ocean
42 biogeochemistry and evolution.

43

44 **Introduction**

45 Viruses represent the most abundant biological entities known on Earth and
46 they are likely to infect any form of life in the ocean (Suttle, 2005; 2007). Over the
47 past decades, it has become evident that viruses play a pivotal role in marine
48 ecosystems, especially through their profound influence on the structure and the
49 functioning of microbial communities (see Brum and Sullivan 2015 for recent
50 review). The ecological impact of viral infection is however largely determined by the
51 different viral life strategies. Lytic viruses replicate and kill their host by cell lysis.
52 This mode of infection influences ocean productivity and biogeochemistry by altering
53 the dynamics, structure, and the function of microbial assemblages (Fuhrman 1999,
54 Suttle 2005) but also the recycling of organic matter through the viral shunt (Fuhrman
55 1999; Wilhelm and Suttle 1999; Brussaard *et al.*, 2008). Lysogenic viruses affect the
56 microbial evolution by inserting their own nucleic sequence into their host genome,
57 which may provide the host with new functional traits and immunity against
58 superinfection (Jiang and Paul 1996; Wilson and Mann 1997). The ecological
59 incidence of chronic infections, by which viruses disseminate by budding or diffusion
60 through host membranes, have been much less documented in marine ecosystems
61 (Thomas *et al.*, 2011; 2012). Despite the global impact of viral infection in the ocean,
62 the regulation of infection dynamics and the relative share among the different
63 infection strategies remain far from understood (Knowles *et al.*, 2016).

64 Several field studies have evidenced latitudinal variations of virus-induced
65 mortality in marine microbial assemblages. For example, increasing viral lysis rates of
66 phytoplankton were recorded from high to low latitudes across the North Atlantic
67 Ocean and, interestingly, correlated positively with temperature and salinity (Mojica
68 *et al.*, 2015). Consistent with this finding, high incidence of lysogeny and low viral

69 lysis rates were shown to occur in low temperature ecosystems such as polar,
70 mesopelagic and deep-sea waters or during cold periods in temperate systems
71 (McDaniel *et al.*, 2002; Williamson *et al.*, 2002; Weinbauer *et al.*, 2003; McDaniel *et*
72 *al.*, 2006; Evans *et al.*, 2009). These studies suggest that viral life strategies other than
73 lytic infection might prevail in cold environments or periods of low productivity.
74 However, other field studies reported contradictory trends (Weinbauer and Suttle
75 1996; Cochran and Paul 1998) and it is still unclear whether temperature driven shifts
76 in viral infection dynamics and strategy represent a global pattern or arise from local
77 processes.

78 Laboratory studies on virus-host model systems in controlled conditions have
79 proven essential to address such fundamental question. These approaches have shown
80 that temperature may influence the infection process by regulating viral abundance
81 and infectivity. Most marine virus isolates tolerate low temperatures whereas
82 increasing temperatures tend to induce loss in infectivity and ultimately inactivation
83 of the viral particles (Nagasaki and Yamagushi, 1998; Baudoux and Brussaard 2005;
84 Tomaru *et al.*, 2005; Martínez-Martínez *et al.*, 2015). Nevertheless, as viruses
85 generally exhibit a broader thermotolerance than their hosts (Mojica and Brussaard
86 2014), and because the optimal temperature for lytic replication (i.e. the temperature
87 that generates fast host lysis and/or high viral yield) generally matches the host
88 optimal growth temperature, it is usually assumed that the impact of temperature on
89 viral infection mostly arises from changes in host metabolism. Temperature driven
90 changes in host physiology were indeed shown to alter the kinetics of viral lysis,
91 possibly inducing the development of viral resistance (Nagasaki and Yamagushi
92 1998; Kendrick *et al.*, 2014; Tomaru *et al.*, 2014) or switches from a lysogenic to lytic
93 lifestyle (Wilson *et al.*, 2001). Altogether, these studies point to important regulatory

94 roles of temperature for viral infection. However, extrapolating results from culture
95 studies to natural ecosystems remains risky given the paucity and the
96 representativeness of the studied virus –host systems.

97 The cosmopolitan picophytoplankter *Micromonas* (Mamiellophyceae,
98 Mamiellales) usually dominates the coastal eukaryotic phytoplankton communities
99 from polar to tropical waters (Thomsen and Buck 1998; Not *et al.*, 2004; Balzano *et*
100 *al.*, 2012; Foulon *et al.*, 2008; Monier *et al.*, 2015). Members of this prominent genus
101 are distributed in 3 discrete genetic clades (Guillou *et al.*, 2004; Foulon *et al.*, 2008)
102 that are all susceptible to viral infection (Martinez-Martinez *et al.*, 2015; Baudoux *et*
103 *al.*, 2015). Previous studies demonstrated that *Micromonas* viruses (MicVs) are
104 ubiquitous, highly dynamic, and induce substantial mortality through cell lysis events
105 in natural and cultured populations (Cottrell and Suttle 1991, 1995; Sahlsten 1998;
106 Zingone *et al.* 1999; Evans *et al.*, 2003; Baudoux *et al.*, 2015). The majority of known
107 MicVs are lytic dsDNA viruses affiliated to the *Phycodnaviridae* family and the
108 genus *Prasinovirus* (Mayer and Taylor 1979; Cottrell and Suttle 1991; Zingone *et al.*
109 2006; Martinez-Martinez *et al.*, 2015), which may represent the most abundant
110 viruses of eukaryotic marine plankton (Hingamp *et al.*, 2013; Yau *et al.*, 2015).
111 *Micromonas* is among the phytoplankters that shows the widest latitudinal distribution
112 on Earth and thereby inhabits waters with contrasted temperatures. Hence,
113 *Micromonas*-virus system constitutes a particularly relevant biological model to
114 investigate how temperature impacts host–virus interactions. To address this problem,
115 we examined the thermal responses of 3 *Micromonas* strains that belong to the three
116 main clades and 3 genetically distinct viruses and monitored the dynamics of the viral
117 infection across a large thermal gradient.

118

119 **Materials and Methods**

120 **Algal and virus culture conditions**

121 *Micromonas* sp. strains RCC451, RCC829 and RCC834 (hereafter referred to
122 as Mic-A, Mic-B and Mic-C; Table 1) that belong to the phylogenetic clades A, B,
123 and C, respectively were retrieved from the Roscoff Culture Collection
124 (<http://roscoff-culture-collection.org/>). Algal cultures were grown in batch conditions
125 in ventilated polystyrene flasks (Nalgene, Rochester, NY, USA) in K-Si medium
126 (Keller *et al.*, 1987). Cultures were maintained under 100 $\mu\text{mol photons m}^{-2} \text{s}^{-1}$ of
127 white light provided by fluorescent tubes (Mazda 18WJr/865) using a 12:12 light:dark
128 cycle, in temperature-controlled chambers at 4, 7.5, 9.5, 12.5, 20, 25, 27.5, 30, and
129 32.5 °C (Aqualytic, Dortmund, Germany). Cultures were thermo-acclimated for
130 several months by multiple serial transfers of early exponentially growing cells.

131 Viral strains RCC4253, RCC4265 and RCC4229 (hereafter referred to as
132 MicV-A, MicV-B and MicV-C) that are lytic to *Micromonas* Mic-A, Mic-B, and
133 Mic-C, respectively, were chosen based on the characterization conducted in Baudoux
134 *et al.* (2015; Table 1). Viral lysates were produced by infecting host cultures grown at
135 20 °C. The model system Mic-B / MicV-B was explored in detail because of its large
136 thermal range.

137

138 **Flow cytometry**

139 All flow cytometric analyses were carried out using a flow cytometer FACS
140 Canto II (Becton Dickinson, San Jose, CA, USA) equipped with an air-cooled argon
141 laser at 488 nm. Green fluorescence intensity (530 nm emission), red fluorescence
142 intensity (emission > 660nm), side scatter (SSC) and forward scatter (FSC) were

143 normalized with standard 0.95 μm fluorescent beads (YG, Polysciences, Warrington,
144 PA, USA).

145 *Micromonas* cell abundances (Figure 1a) were determined using the SSC and
146 the red fluorescence signals. The samples were analysed for 1 min at the appropriate
147 flow speed according to culture concentration in order to avoid coincidence events
148 (Marie *et al.*, 1999). The growth rates of *Micromonas* Mic-A, Mic-B and Mic-C
149 acclimated from 4 to 30 $^{\circ}\text{C}$ were computed as the slope of $\ln(Nt)$ vs. time plot, where
150 Nt is the cell number at time t . All measurements were done on at least 4 replicates.

151 In addition, cell membrane permeability, used as a proxy for viability, was
152 monitored by flow cytometry using SYTOX-Green. This dye is a membrane-
153 permeant nucleic acid probe (Life Technologies, Saint-Aubin, France), that only
154 binds to nucleic acids of cells that have compromised membranes. SYTOX-Green (0.5
155 μM final concentration) was added to fresh sample and the mixture was incubated for
156 5 min in the dark at the corresponding growth temperature (Peperzak and Brussaard
157 2011). Cells with compromised membranes were discriminated based on their higher
158 green fluorescence (Figure 1b).

159 Viral abundances were determined on glutaraldehyde fixed samples (0.5%
160 final concentration, Grade II, Sigma Aldrich, St Louis, MO, USA) stored at -80 $^{\circ}\text{C}$
161 until analysis. Flow cytometry analysis was performed as described by Brussaard
162 (2004). Briefly, samples were thawed at 37 $^{\circ}\text{C}$, diluted in 0.2 μm filtered autoclaved
163 TE buffer (10:1 Tris-EDTA, pH = 8) and stained with SYBR-Green I (concentration,
164 Life Technologies, Saint-Aubin, France) for 10 minutes at 80 $^{\circ}\text{C}$. Virus particles were
165 discriminated based on their green fluorescence and SSC during 1 min analyses
166 (Figure 1c). All cytogram analyses were performed with the Flowing Software
167 freeware (Turku Center of Biotechnology, Finland).

168

169 ***Micromonas* growth rate modelling**

170 A Cardinal Temperature Model with Infection (CTMI model) relying on
171 experimental growth rates was used to calculate the optimal growth temperature
172 (T_{opt}), for which growth rate is optimal (μ_{opt}), and the minimal and maximal growth
173 temperatures (T_{min} and T_{max}) beyond which growth rate is assumed to be zero
174 (Bernard and Rémond, 2012). The determination of these parameters was essential to
175 select the appropriate temperature for infection experiments. Cardinal temperatures
176 (T_{min} , T_{opt} , and T_{max}) of *Micromonas* and thermal growth response were predicted
177 using the relation:

$$\mu_{max} = \begin{cases} 0 & \text{for } T < T_{min} \\ \mu_{opt} \cdot \phi(T) & \text{for } T_{min} < T < T_{max} \\ 0 & \text{for } T > T_{max} \end{cases}$$

178 Where $\phi(T) = \frac{(T-T_{max})(T-T_{min})^2}{(T_{opt}-T_{min})[(T_{opt}-T_{min})(T-T_{opt})-(T_{opt}-T_{max})(T_{opt}+T_{min}+2T)]}$

179 The same algorithm was used in Bernard and Rémond (2012) to identify
180 model parameters and the confidence intervals were determined with a jackknife
181 method with a 95% threshold.

182

183 **Pulse Amplitude Modulated fluorimetry**

184 The quantum yield of photosystem II of algal cells was determined using a
185 pulse amplitude modulated fluorometer (Phyto-PAM, Walz) connected to a chart
186 recorder (Labpro, Vernier) in order to monitor the impact of temperature and viral
187 infection on host photophysiology. After 5 min relaxation in darkness, the non-actinic
188 modulated light (450 nm) was turned on in order to measure the fluorescence basal
189 level, F_0 . A saturating red light pulse (655 nm, 4 000 $\mu\text{mol quanta m}^{-2} \text{s}^{-1}$, 400 ms)
190 was applied to determine the maximum fluorescence level in the dark-adapted sample,

191 F_M . The maximal photosystem II fluorescence quantum yield of photochemical energy
192 conversion, F_V/F_M , was calculated using the following formula:

$$\frac{F_V}{F_M} = \frac{(F_M - F_0)}{F_M}$$

193

194 **Measuring the effect of temperature on virion infectivity and abundance**

195 Freshly produced 0.2 μm filtered (Polyethersulfone membrane) viral lysates of
196 MicV-A, MicV-B and MicV-C were diluted in K-Si culture medium to a final
197 concentration of 10^6 viral particles mL^{-1} . Aliquots of these viral suspensions were
198 incubated in darkness at 4, 7.5, 12.5, 20, 25, 27.5, 30 $^{\circ}\text{C}$, which corresponds to the
199 global temperature range encountered in the ocean. Samples for total virus abundance
200 and infectivity were taken once a week and once every two weeks, respectively,
201 during 6 weeks. Viral abundance was monitored by flow cytometry as described
202 above. Viral infectivity was assessed using end-point dilution method (Most Probable
203 Number method MPN; Taylor, 1962). To this end, virus suspensions were serially
204 diluted (10-fold increments) in exponentially growing *Micromonas* cultures in 48-
205 multiwell plates and incubated at 20 $^{\circ}\text{C}$ for 10 days. Each serial dilution was done in
206 triplicate along with a control, non-infected *Micromonas* culture. After incubation, the
207 cultures that underwent lysis, as seen by the colour change, were counted and the
208 infectious virus concentration was determined with the software *Most Probable*
209 *Number* (MPN; version 2.0, Avineon, U.S Environmental Protection Agency).

210

211 Particle degradation and decrease in infectivity rates (respectively d_s and d_i)
212 were calculated from viral counts and viral infectivity measurements as follows:

$$213 \quad d_s = \frac{\ln(V_{t+1}) - \ln(V_t)}{t_{+1} - t},$$

214 Where V_{t+1} and V_t are the concentration of viral particles at time t_{+1} and t ,
215 respectively, and:

$$d_i = \frac{\ln(I_{t+1}) - \ln(I_t)}{t_{+1} - t}$$

216 Where I_{t+1} and I_t are the concentrations of infectious viral particles at time t_{+1} and t ,
217 respectively.

218

219 **Measuring the effect of temperature on the *Micromonas*-virus interactions**

220 The effects of temperature on virus-host interactions were assessed by infection
221 dynamics experiments. For the model system Mic-B / MicV-B, host cultures
222 acclimated at 9.5, 12.5, 20, 25, 27.5 and 30 °C were prepared at a concentration of $5 \times$
223 10^5 cell mL^{-1} and split into four sub-cultures. Three of the sub-cultures were infected
224 with a fresh, 0.2 μm -filtered virus lysate of MicV-B at a multiplicity of infection
225 (MOI) of 10. The fourth culture, uninfected, served as control. Control and infected
226 cultures, incubated at each temperature, were sampled every 3 to 4 hours during 120
227 hours for measurements of host and viral abundances, host cell membrane integrity
228 and photosynthetic capacity (see above).

229 Three viral parameters, the latent period, the viral production, and, when applicable,
230 the burst size, were calculated from viral growth cycle. The latent period was
231 calculated as the lapse-time between inoculation of viruses in host culture and the
232 release of viral particles by host cells. A viral production rate was calculated as the
233 slope of the logarithm curve of viral concentration over time following the equation:

$$\text{viral production rate} = \frac{\ln(V_{t+1}) - \ln(V_t)}{\Delta_t}$$

234 With V_{t+1} the viral concentration at time t_{+1} and V_t the viral concentration at time t for
235 the period $\Delta_t = t_{+1} - t \leq 24 \text{ h}$.

236 If complete host lysis occurred, the burst size (BS) was calculated as the number of
237 viral particles produced per infected host cell as:

$$BS = \frac{V_{\max} - V_0}{H_{\max} - H_{\min}}$$

238 Where V_0 is the viral concentration and T_0 , V_{\max} the maximum concentrations of viral
239 particles during the experiment, and H_{\max} and H_{\min} the maximal and minimal host
240 abundances during the experiment.

241

242 For the model systems Mic-A / MicV-A and Mic-C / MicV-C, a simplified
243 experimental setup and sampling strategy were used. Infection cycles were monitored
244 at only five temperatures: 12.5, 20, 25, 27.5 and 30 °C. Infections at 12.5, 20, 27.5
245 and 30 °C were sampled every 10 - 14 hours during 120 hours for host and virus
246 abundance and photosynthetic capacity measurements. Infections at 25 °C were
247 sampled for host and virus abundance every 3 – 4 hours during 28 hours and every 12
248 hours for the remaining 96 hours.

249

250 **Results**

251 **Effect of temperature on *Micromonas* growth**

252 The growth rate of *Micromonas* sp. strains Mic-A, Mic-B and Mic-C was
253 measured at temperatures ranging from 4 to 32.5 °C (Figure 2 – Table 2). The growth
254 responses to temperature followed a typical, asymmetric bell-shaped curve over the
255 selected temperature range with an asymptotic increase at temperatures below T_{opt} and
256 an abrupt decline at temperatures beyond T_{opt} . CTMI model fitting resulted in the
257 determination of optimum growth temperature (T_{opt}) values of 25.1, 26.7, and 24.3 °C
258 for Mic-A, Mic-B, and Mic-C, respectively. Mic-A and Mic-C showed a similar

259 optimal growth rate ($\mu_{\text{opt}} = 0.8 \text{ d}^{-1}$), while Mic-B ($\mu_{\text{opt}} = 1.1 \text{ d}^{-1}$) was higher.
260 *Micromonas* strain Mic-B exhibited the largest thermal range with a theoretical T_{min}
261 of $0.55 \text{ }^{\circ}\text{C}$ and T_{max} of $32.5 \text{ }^{\circ}\text{C}$. Mic-A and Mic-C appeared slightly more restrictive
262 with a positive growth between 9.6 and $32.5 \text{ }^{\circ}\text{C}$ and $5.7 - 30.1 \text{ }^{\circ}\text{C}$, respectively. Based
263 on these thermal responses, we investigated the stability of the virus particles and the
264 potential changes in the virus - host interactions below or at T_{opt} (7.5 or 9.5 , 12.5 , 20
265 $^{\circ}\text{C}$ and $25 \text{ }^{\circ}\text{C}$) and beyond T_{opt} (27.5 and $30 \text{ }^{\circ}\text{C}$).

266

267 **Thermal stability of *Micromonas* virions**

268 The thermal stability of the viral particles MicV-A, MicV-B and MicV-C was
269 investigated over a 6-week period, during which viral infectivity and particle integrity
270 were monitored. Rates of decay for these two parameters varied considerably among
271 the three viral strains (Figure 3). MicV-C was the most stable over the range of
272 selected temperature. MicV-C infectivity and particle integrity both declined at
273 similar rates between $7.5 \text{ }^{\circ}\text{C}$ ($0.08 \pm 0.05 \text{ d}^{-1}$) and $27.5 \text{ }^{\circ}\text{C}$ ($0.1 \pm 0.02 \text{ d}^{-1}$), while
274 infectivity decay rates increased considerably only at $30 \text{ }^{\circ}\text{C}$ ($0.35 \pm 0.02 \text{ d}^{-1}$). The
275 infectivity decay rates were globally higher for MicV-A and MicV-B virions,
276 increasing gradually (from $0.17 \pm 0.025 \text{ d}^{-1}$ to $0.44 \pm 0.01 \text{ d}^{-1}$) with increasing
277 temperature. In spite of these considerable losses in infectivity, total counts of viral
278 particles decreased at much lower rates, suggesting that MicV-A and MicV-B had
279 lost the ability to infect their hosts prior to particle destruction.

280

281 **Impact of temperature on virus - host interactions**

282 Infection dynamics experiments revealed that virus – host interactions were
283 strongly affected by temperature, but each virus-host systems displayed distinct
284 responses (Figures 4 and 6).

285

286 **Mic-B / MicV-B**

287 Both infection kinetics and the fate of the infected *Micromonas* cells differed
288 between temperature treatments. Below Mic-B T_{opt} (25, 20, 12.5, and 9.5 °C), MicV-
289 B propagated through a typical lytic cycle (Figure 4). The virus latent period
290 increased progressively with decreasing temperature ranging from < 3 h at 25 °C to
291 the 7 – 11 h at 12.5 and 9.5 °C (Figures 4a - d). Similarly, the rates of virus
292 production was substantially faster at 25 and 20 °C (5.76 and 5.52 d⁻¹, Figures 4c, 4d)
293 compared to that at 9.5 and 12.5 °C (0.48 and 0.96 virus produced d⁻¹, respectively,
294 Figures 4a, 4b). The virus production at 25 and 20 °C induced host cell lysis, which
295 was accompanied by a disruption of host membranes (Figures 4o, 4p, Supplementary
296 Figure 1) and a decrease in photosynthetic capacity (Figures 4v, 4w). The resulting
297 burst size (139 to 142 virions host⁻¹) was comparable for both temperature treatments.
298 At 12.5 °C and 9.5 °C, the host cell lysis was delayed considerably. At these
299 temperatures, control and infected cultures displayed similar growth rates (Figures 4g,
300 4h) and neither the host membrane integrity (Figures 4m, 4n) nor the photosynthetic
301 capacity (Figures 4s, 4t) appeared to be altered by the virus production until 70 h post-
302 infection. The loss in host abundance recorded 70 h post infection (Figures 4g, 4h) led
303 to estimate a burst size of 84 virions host⁻¹ at 12.5 °C. At 9.5 °C, the infected host
304 abundance did not decline during the 120 hours sampling, precluding calculation of
305 the burst size. Lysis of infected host was nevertheless confirmed by a visual control
306 (the infected culture became transparent) at 140 hours post-infection.

307 At temperatures above T_{opt} (27.5 and 30 °C), complete host cell lysis was not
308 observed and viral infections appeared to follow a two-step process. At 27.5 °C, virus
309 infection led to a rapid release of viral progeny (latent period < 3 h) at a substantial
310 production rate (6.24 d^{-1}) until a plateau in virus concentration was reached after 20 h
311 (Figure 4e). A second increase in viral abundance with a production rate of 0.48 d^{-1}
312 was recorded from after 70 h, which was maintained until the end of the experiment.
313 Interestingly, viral infection at 27.5 °C did not result in complete collapse of the host
314 culture (Figure 4k, Supplementary Figure 1). A slight decline in infected host cell
315 abundance (Figure 4k), membrane integrity (from 100 to 90%, Figure 4q) and F_V/F_M
316 (from 0.55 to 0.45, Figure 4x) accompanied the first viral burst (BS of 177 virions
317 host^{-1}). However, the second production of viruses did not induce cell lysis. Indeed,
318 infected host cells grew at slower rates than control cultures (0.62 d^{-1} compared to
319 1.11 d^{-1} ; Figure 4k), yet they exhibited unaltered membrane integrity (Figure 4q) and
320 F_V/F_M (Figure 4x) compared to the control. The estimation of the viral BS was not
321 possible in absence a host cell lysis; instead we calculated a viral release of 5 virions
322 $\text{cell}^{-1} \text{ d}^{-1}$.

323 Last, virus infection at 30 °C resulted in a reduced production rate of viral
324 progeny (3.6 d^{-1}) after a latent period of 3 to 7 h and a gradual decay in viral
325 abundance from 35 h until the end of the experiment (Figure 4f). As observed at 27.5
326 °C, the viral production was accompanied by an incomplete host cell lysis (Figure 4l,
327 Supplementary Figure 1). The production of viral progeny and subsequent cell lysis
328 induced slight declines in infected host cell abundance, membrane integrity (from 100
329 to 90%, Figure 4r) and F_V/F_M (from 0.55 to 0.45, Figure 4y). The resulting viral BS
330 reached 49 virions host^{-1} . Yet, we observed a regrowth of infected host at a rate of
331 0.81 d^{-1} (compared to 0.69 d^{-1} for the control) after 80 h (Figure 4l) and restoration of

332 membrane integrity and photosynthetic capacity after 27 h until the end of the
333 experiment (Figure 4 r and 4y).

334 Altogether, these results indicate that rates of viral production were positively
335 related to host growth rate whereas viral latent period was inversely related to the host
336 growth rates (Figure 5). Optimal viral replication (shortest latent period and fastest
337 viral production) occurred at a temperature between 25 and 27.5 °C, which
338 correspond to the optimal growth of *Micromonas* Mic-B.

339

340 **Mic-A / MicV-A and Mic-C / MicV-C**

341 As observed for MicV-B, MicV-A and MicV-C replicated through a typical
342 lytic cycle only below host T_{opt} (20 and 12.5 °C, Figure 6). At 20 °C, viruses were
343 released after latent periods lower than 14 h and 14 to 24 h for MicV-A and MicV-C,
344 respectively, with virion production rates of 2.64 and 1.44 d⁻¹, respectively. The
345 strong decrease in cell abundance in the infected cultures indicates that viral
346 production induced complete collapse of the corresponding host culture (Figure 6f,
347 Supplementary Figure 2). The resulting BS reached values of 130 – 158 virions host⁻¹
348 and 177 – 197 virions host⁻¹ for MicV-A and MicV-C, respectively (Figure 6b). At
349 12.5 °C, MicV-A and MicV-C readily propagated in their respective host; yet the
350 duration of virus latent periods were prolonged (19 – 29 h) compared to the 20 °C
351 treatment with virion production rates of 1.2 and 0.96 d⁻¹, respectively (Figure 6a).
352 The release of viral progeny was accompanied by immediate host lysis and the
353 resulting burst size was reduced for MicV-A and MicV-C (57 – 69 and 80 – 96
354 virions host⁻¹ respectively) compared to infection at 20 °C (Figure 6e, Supplementary
355 Figure 2).

356 At temperatures close to T_{opt} (25 °C), infection by MicV-A and MicV-C did
357 not result in cell lysis while viruses were still produced (Figure 6c and g,
358 Supplementary Figure 2). The duration of the virus latent periods was similar (7 – 11h
359 and 27 – 31h) compared to the 20 °C treatment with virion production rates of 0.48
360 and 0.84 d^{-1} , respectively. The resulting growth rate of infected Mic-A cells was not
361 different to the control (0.8 d^{-1}) whereas infected Mic-C grew at a lower rate than the
362 control (0.36 vs. 1.02 d^{-1}).

363 At temperatures beyond host T_{opt} (27.5 and 30 °C), infection by MicV-A and
364 MicV-C did not result in any production of viruses. Infected *Micromonas* cells were
365 apparently not altered by the presence of viruses, growing at rates similar to control
366 cultures (Figure 6d, e, h, i) with unaffected photosynthetic yields (data not shown).
367

368 Discussion

369 The response of *Micromonas* strains to temperature is typical for a
370 eurythermal mesophilic species, characterized by a wide range of thermal tolerance
371 with an optimal growth temperature (T_{opt}) between 20 and 25 °C. Deviation from the
372 optimal growth temperature is thought to induce modifications of intrinsic
373 biochemical and physiological functions in order to optimize resource allocation for
374 growth on the one hand, and to maintain cell integrity on the other hand (Ras *et al.*,
375 2013; Behrenfeld *et al.*, 2008). As a result, *Micromonas* growth response below T_{opt}
376 reflects cold acclimation whereas the abrupt decline of growth rates beyond T_{opt}
377 suggests dramatic deleterious effects of heat on cellular components (Raven and
378 Geider 1988; Ras *et al.*, 2013; Dill *et al.*, 2011). Although the three *Micromonas*
379 strains exhibited broad temperature tolerances, the strain belonging to clade B (Mic-
380 B) showed the largest thermal tolerance range (from 0.55 – 32.5 °C) while strains
381 belonging to clades A and C were more restrictive with thermal tolerance ranging
382 from 9.6 to 32.5 °C and from 5.7 to 30.1 °C, respectively. Whether these differences
383 are generally the case for all of the members of these clades remains to be
384 investigated. To the best of our knowledge, no study has explored the existence of
385 thermotypes in *Micromonas* species. Nonetheless, our results suggest that the selected
386 *Micromonas* strains might have evolved divergent acclimation strategies, which may,
387 in turn, influence virus-host interactions.

388 The detailed study of the model system Mic-B / MicV-B unequivocally
389 demonstrated that viral infection is altered by temperature. At temperatures lower than
390 T_{opt} , MicV-B propagated and killed their hosts through cell lysis as classically
391 reported in the literature (Mayer and Taylor 1979, Zingone *et al.* 2006; Baudoux *et al.*
392 2015; Martinez-Martinez *et al.*, 2015). Yet the kinetics and the intensity of viral

393 replication slowed down with decreasing temperatures. MicV-B propagated the most
394 efficiently at 25 °C, which corresponded to a temperature close to the optimal growth
395 temperature of *Micromonas* sp. Mic-B. Under these growth conditions, MicV-B
396 readily adsorbed on host membranes and rapidly hijacked host cellular machinery for
397 viral DNA replication as well as virion protein synthesis and assembly, as indicated
398 by the short latent period (< 3 h), the high burst size (140) and the fast viral
399 production rate (5.5 d⁻¹). The observed viral parameters fall within the range of
400 reported values for other *Micromonas* viral isolates (Mayer and Taylor 1979;
401 Baudoux and Brussaard 2008; Baudoux *et al.*, 2015). Decrease in temperature led to
402 increased latent periods and the coldest temperatures (12.5 and 9.5 °C) also induced a
403 reduction of viral production rates and a substantial delay in host cell lysis. The
404 relatively low viral decay rates recorded across this thermal range indicated that
405 MicV-B particles did remain infectious under these conditions. It is thus likely that
406 the acclimation strategy evolved by Mic-B to grow at temperatures below T_{opt} was
407 responsible for the alteration of the viral infection process. The decrease in auto-
408 fluorescence intensity of cold-adapted *Micromonas* (Supplementary Figure 3)
409 suggests a reduction in chlorophyll content with decreasing temperatures as
410 previously reported (Claquin *et al.*, 2008). Several studies pointed out the similarity of
411 photoacclimation trends at low temperatures to those at high irradiance (Anning *et al.*,
412 2001, El-Sabaawi and Harrison 2006, Claquin *et al.*, 2008). Reports on the effect of
413 light intensity evidenced the importance of this factor in regulating algal host – virus
414 interactions (Waters and Chan 1982; Bratbak *et al.*, 1998; Brown *et al.*, 2007;
415 Baudoux and Brussaard 2008). However, elevated irradiance *per se* did not appear to
416 alter viral infection of *Micromonas* (Baudoux and Brussaard 2008). Several other
417 reasons might explain changes in viral infection of Mic-B at low temperatures. For

418 example, low temperatures were shown to slow down the rates of translation initiation
419 at the ribosome site in phytoplankton (Toseland *et al.*, 2013). The globally reduced
420 metabolic activities and protein biosynthesis may thus result in a slower synthesis and
421 assembly of virions proteins, which, in turn, could explain the decrease in viral
422 progeny production. Another known impact of low temperatures is the stiffening of
423 phytoplankton membranes through the activation of lipid desaturases (Los and Murata
424 2004; D'Amico *et al.*, 2006). Interestingly, the monitoring of *Micromonas* membrane
425 integrity indicated a modification of their membrane properties. While cell division
426 enhanced membrane permeability at 25 and 20 °C, host membranes remained
427 impermeable to the dye throughout their cell cycle at the coldest temperatures (9.5
428 and 12 °C), supporting the idea that Mic-B membranes became more rigid. Such
429 modification might not only impact viral adsorption on host cell, which would result
430 in a prolonged latent period, but it may also delay the release of viral progeny and,
431 thereby, the timing of host lysis.

432 Notably, temperatures above T_{opt} altered the algicidal activity of *Micromonas*
433 viruses considerably. A 1°C temperature increase beyond T_{opt} induced host tolerance
434 to viral infection. At 27.5 °C, we indeed observed a rapid transition from a classical
435 lytic infection mode to a viral life strategy reminiscent of chronic infection, by which
436 viruses are released with no apparent sign of host lysis. This infection mode has never
437 been reported in MicV. Yet, one of the few examples of chronic infection in marine
438 systems has interestingly been described for another prasinovirus that infects the
439 green alga *Ostreococcus tauri*, a close relative of *Micromonas* sp. (Thomas *et al.*,
440 2011). *Ostreococcus* virus OtV-5 switched from a lytic to a chronic lifestyle within a
441 few days of incubation, after lysis of most of the host cells remaining host cells were
442 resistant but produced viruses chronically. The viral yield of chronically infected cells

443 is within the same range for both model systems with 1–3 and 5 viruses host⁻¹ day⁻¹ in
444 *Ostreococcus* and *Micromonas*, respectively. Yet, the growth rate of chronically
445 infected *Micromonas* cells was considerably reduced while no reduction in growth
446 rate was evidenced in *Ostreococcus* species (Thomas *et al.*, 2011). As argued for
447 lysogeny, chronic infection ensures a co-existence between host and virus in
448 unfavourable conditions (e.g. low host density, sub-optimal growth environments,
449 Thomas *et al.*, 2012; Mackinder *et al.*, 2009). Being in the vicinity of their host may
450 directly benefit the virus if growth conditions improved. The mechanisms that trigger
451 a lytic – chronic decision remain to be established. Our results however suggest that
452 this switch in life strategy did not operate when temperatures deviated excessively
453 from the growth optimum. At 30 °C, MicV-B rapidly replicated through cell lysis and
454 regrowth of infected *Micromonas* cells was recorded following this lytic event as
455 observed at 27.5 °C. A number of interpretations could explain the findings of low
456 viral production and continued host growth at 30°C. The observed loss of viral
457 infectivity at this temperature suggests that viruses could become inactive during the
458 period of the experiment. However, we cannot rule out that alterations of host
459 phenotype modify their susceptibility to viral infection as demonstrated recently in
460 Kendrick *et al.* (2014). Hence, temperatures above T_{opt} induced complex outcomes
461 after viral infection in Mic-B. Importantly, chronic infections might arise more
462 frequently than previously thought, at least among marine prasinophytes.

463 The investigation of two additional *Micromonas* – virus systems suggests that
464 the previously observed temperature effects on the viral infection process are not
465 specific to the model system Mic-B / MicV-B. Despite the variable thermal tolerance
466 of the studied *Micromonas* hosts and their respective viruses, temperature affected the
467 outcome of viral infections similarly. Infection dynamics experiments demonstrated

468 that temperatures below T_{opt} slowed down the kinetics and intensity of the lytic cycle
469 while temperatures close to and higher than T_{opt} induced complex outcomes in viral
470 infections. Infections at 25 °C might correspond to temperature slightly above T_{opt} as
471 the averaged predicted T_{opt} were 25.1 °C (24.5 – 25.8) and 24.3 °C (23.4 – 25.2) for
472 Mic-A and Mic-C, respectively. As observed previously, a slight increase beyond T_{opt}
473 induced a viral life strategy reminiscent of chronic infection while excessive deviation
474 from T_{opt} inhibited viral production, although hosts maintained their ability to grow.
475 Hence, the thermal environment of *Micromonas* determines the outcome of viral
476 infection, leading to drastic changes in the lytic cycle and a possible switch in viral
477 life strategy. Similar thermal responses to viral infection were reported for the
478 raphidophyte *Heterosigma akashiwo* (Nagazaki and Yamagushi 1998) and the
479 haptophyte *Emiliana huxleyi* (Kendrick *et al.*, 2014). An alteration of the algicidal
480 activity of viruses at high temperatures and a reduced intensity of viral lysis at low
481 temperatures seem to represent a global pattern, which may have important
482 consequences for the regulation of phytoplankton population in the ocean.

483 Because of their worldwide distribution and persistence in marine systems,
484 *Micromonas* and their viruses are exposed to important changes in environmental
485 parameters, including temperature. Results of this study clearly demonstrated that a 1
486 °C change can profoundly affect the outcome of viral infection and can even lead to
487 development of complex outcomes of viral lysis. It is thus very likely that temperature
488 contributes to the control of viral induced mortality in *Micromonas* populations both
489 at a temporal and a geographical scale. There is, to our knowledge, no report of actual
490 viral lysis rates in *Micromonas* natural populations to support our speculation.
491 Nonetheless, a recent study observed a latitudinal variation in virus-mediated
492 mortality of phytoplankton across the North Atlantic Ocean and pointed out a

493 correlation between the velocity of viral lysis and *in situ* temperature that varied
494 between 10 – 25 °C (Mojica *et al.*, 2015). Such geographic partitioning of viral lysis
495 processes could have important consequences for the ecology and the
496 biogeochemistry of the global ocean. Viral lysis diverts phytoplankton biomass away
497 from the higher trophic level towards the microbial loop through the release of
498 cellular compounds upon host cell lysis. Temperature-driven changes in the amount of
499 viral-mediated mortality and in host cell stoichiometry (due to changes in biochemical
500 functions) could thereby alter the structure of marine food webs and the capacity of
501 pelagic systems to sequester carbon. Given the anticipated increase of sea surface
502 temperature due to global warming, it is essential to gain a better understanding of the
503 thermal response and life strategy in other prominent virus – phytoplankton model
504 systems. Such studies are necessary for improving ecosystem models in ecosystem-
505 based considerations of climate change.

506

507 Supplementary information is available at ISMEJ's website.

508

509 **Acknowledgments**

510 We grateful to the MICROBIOL Master students 2015-2016 for repeating infection
511 dynamics experiments and to Nigel Grimsley, Hervé Moreau, and Evelyne Derelle for
512 stimulating discussion. We thank the three anonymous reviewers for their
513 constructive comments on a previous version of this manuscript. This research was
514 funded by the ANR funding agency REVIREC; grant no. 12-BSV7-0006-01.

515

516 **Conflict of interest statement**

517 Authors declare no conflict of interest for this study

518 **Bibliography**

519

520 Anning T, Harris G, Geider R. (2001). Thermal acclimation in the marine diatom
521 *Chaetoceros calcitrans* (Bacillariophyceae). *European Journal of Phycology* **36**: 233-
522 241.

523 Balzano S, Marie D, Gourvil P, Vaultot D. (2012). Composition of the summer
524 photosynthetic pico and nanoplankton communities in the Beaufort Sea assessed by
525 T-RFLP and sequences of the 18S rRNA gene from flow cytometry sorted samples.
526 *The ISME Journal* **6**: 1480-1498.

527 Baudoux A-C, Brussaard CPD. (2005). Characterization of different viruses infecting
528 the marine harmful algal bloom species *Phaeocystis globosa*. *Virology* **341**: 80-90.

529 Baudoux A-C, Brussaard CPD. (2008). Influence of irradiance on virus-algal host
530 interactions. *Journal of Phycology* **44**: 902-908.

531 Baudoux A-C, Lebretonchel H, Dehmer H, Latimier M, Edern R, Rigaut-Jalabert F,
532 *et al.* (2015). Interplay between the genetic clades of *Micromonas* and their viruses in
533 the Western English Channel. *Environmental Microbiology Reports* **44**: 765-773.

534 Behrenfeld MJ, Halsey KH, Milligan AJ. (2008). Evolved physiological responses of
535 phytoplankton to their integrated growth environment. *Philosophical Transactions of*
536 *the Royal Society B: Biological Sciences* **363**: 2687-2703.

537 Bellec L, Grimsley N, Moreau H, Desdevises Y. (2009). Phylogenetic analysis of new
538 Prasinoviruses (Phycodnaviridae) that infect the green unicellular algae *Ostreococcus*,
539 *Bathycoccus* and *Micromonas*. *Environmental Microbiology Reports* **1**: 114-123.

540 Bellec L, Grimsley N, Derelle E, Moreau H, Desdevises Y. (2010). Abundance,
541 spatial distribution and genetic diversity of *Ostreococcus tauriviruses* in two different
542 environments. *Environmental Microbiology Reports* **2**: 313-321.

543 Bernard O, Rémond B. (2012). Validation of a simple model accounting for light and
544 temperature effect on microalgal growth. *Bioresource Technology* **123**: 520-527.

545 Bratbak G, Heldal M, Thingstad TF, Riemann B, Haslund OH. (1998). Viral lysis of
546 *Phaeocystis pouchetii* and bacterial secondary production. *Aquatic Microbial Ecology*
547 **16**: 11-16.

548 Brown CM, Campbell DA, Lawrence JE. (2007). Resource dynamics during infection
549 of *Micromonas pusilla* by virus MpV-Sp1. *Environmental Microbiology* **9**: 2720-
550 2727.

551 Brum JR, Sullivan MB. (2015). Rising to the challenge: accelerated pace of discovery
552 transforms marine virology. *Nature Reviews Microbiology* **13**: 147-159.

- 553 Brussaard CPD. (2004). Viral Control of Phytoplankton Populations-a Review.
554 *Journal of Eukaryotic Microbiology* **51**: 125-138.
- 555 Brussaard C, Martinez JM. (2008). Algal bloom viruses. *Plant Viruses* **2**: 1-13.
- 556 Campbell D, Hurry V, Clarke AK. (1998). Chlorophyll fluorescence analysis of
557 cyanobacterial photosynthesis and acclimation. *Microbiology and Molecular Biology*
558 *Reviews* **62**: 667-683.
- 559 Chen B. (2015). Patterns of thermal limits of phytoplankton. *Journal of Plankton*
560 *Research* **37**: 285-292.
- 561 Claquin P, Probert I, Lefebvre S. (2008). Effects of temperature on photosynthetic
562 parameters and TEP production in eight species of marine microalgae. *Aquatic*
563 *Microbial Ecology* **51**: 1-11.
- 564 Cochran P, Paul J. (1998). Seasonal abundance of lysogenic bacteria in a subtropical
565 estuary. *Applied and Environmental Microbiology* **64**: 2308-2312.
- 566 Cottrell MT, Suttle CA. (1991). Wide-spread occurrence and clonal variation in
567 viruses which cause lysis of a cosmopolitan, eukaryotic marine phytoplankter. *Marine*
568 *Ecology Progress Series* **78**: 1-9.
- 569 Cottrell MT, Suttle CA. (1995). Dynamics of lytic virus infecting the photosynthetic
570 marine picoflagellate *Micromonas pusilla*. *Limnology Oceanography* **40**: 730-739.
- 571 D'Amico S, Collins T, Marx J-C, Feller G, Gerday C. (2006). Psychrophilic
572 microorganisms: challenges for life. *EMBO Reports* **7**: 385-389.
- 573 Dill K, Ghosh K & Schmit J (2011). Physical limits of cells and proteomes.
574 *Proceedings National Academy of Science USA* **108**: 17876-17882.
- 575 El-Sabaawi R, Harrison PJ. (2006). Interactive effects of irradiance and temperature
576 on the photosynthetic physiology of the pennate diatom pseudo - nitzschia granii
577 (bacillariophyceae) from the northeast subarctic pacific. *Journal of Phycology* **42**:
578 778-785.
- 579 Evans C, Archer SD, Jacquet S, Wilson WH. (2003). Direct estimates of the
580 contribution of viral lysis and microzooplankton grazing to the decline of a
581 *Micromonas* spp. population. *Aquatic Microbial Ecology* **30**: 1-13.
- 582 Evans C, Pond DW, Wilson WH. (2009). Changes in *Emiliana huxleyi* fatty acid
583 profiles during infection with E-huxleyi virus 86: physiological and ecological
584 implications. *Aquatic Microbial Ecology* **55**: 219-228.
- 585 Foulon E, Not F, Jalabert F, Cariou T, Massana R, Simon N. (2008). Ecological niche
586 partitioning in the picoplanktonic green alga *Micromonas pusilla*: evidence from
587 environmental surveys using phylogenetic probes. *Environmental Microbiology* **10**:
588 2433-2443.
- 589 Fuhrman JA. (1999). Marine viruses and their biogeochemical and ecological effects.
590 *Nature* **399**: 541-548.

- 591 Guillou L, Eikrem W, Chrétiennot-Dinet M-J, Le Gall F, Massana R, Romari
592 Khadidja, Pedros-Alio C, Vaultot D. (2004). Diversity of picoplanktonic prasinophytes
593 Assessed by direct nuclear SSU rDNA sequencing of environmental samples and
594 novel isolates retrieved from oceanic and coastal marine ecosystems. *Protist* **155**:
595 193-214.
- 596 Hingamp P, Grimsley N, Acinas SG, Clerissi C, Subirana L, Poulain J, *et al.* (2013).
597 Exploring nucleo-cytoplasmic large DNA viruses in Tara Oceans microbial
598 metagenomes. *The ISME Journal* **7**: 1678-1695.
- 599 Jiang SC, Paul JH. (1996). Occurrence of lysogenic bacteria in marine microbial
600 communities as determined by prophage induction. *Marine Ecology Progress Series*
601 **35**: 235-243.
- 602 Keller MD, Selvin RC, Claus W, Guillard RRL. (1987). Media for the culture of
603 oceanic ultraphytoplankton. *Journal of Phycology* **23**: 633-638.
- 604 Kendrick BJ, DiTullio GR, Cyronak TJ, Fulton JM, Van Mooy BAS, Bidle KD.
605 (2014). Temperature-Induced Viral Resistance in *Emiliania huxleyi*
606 (*Prymnesiophyceae*). *PLoS ONE* **9**: e112134-14.
- 607 Knowles B, Silveira CB, Bailey BA, Barott K, Cantu VA, Cobián-Güemes AG, *et al.*
608 (2016). Lytic to temperate switching of viral communities. *Nature* **531**: 466-470.
- 609 Los DA, Murata N. (2004). Membrane fluidity and its roles in the perception of
610 environmental signals. *Biochimica et Biophysica Acta (BBA) - Biomembranes* **1666**:
611 142-157.
- 612 Mackinder LCM, Worthy CA, Biggi G, Hall M, Ryan KP, Varsani A, *et al.* (2009). A
613 unicellular algal virus, *Emiliania huxleyi* virus 86, exploits an animal-like infection
614 strategy. *Journal of General Virology* **90**: 2306-2316.
- 615 Marie D, Brussaard C, Thyrhaug R, Bratbak G, Vaultot D. (1999). Enumeration of
616 marine viruses in culture and natural samples by flow cytometry. *Applied and*
617 *Environmental Microbiology* **65**: 45-52.
- 618 Martínez Martínez J, Boere A, Gilg I, Lent J W M V, Witte HJ, Bleijswijk J D L V, *et*
619 *al.* (2015a). New lipid envelop-containing dsDNA virus isolates infecting
620 *Micromonas pusilla* reveal a separate phylogenetic group. *Aquatic Microbial Ecology*
621 **74**: 17-28.
- 622 Mayer JA, Taylor FJR. (1979). A virus which lyses the marine nanoflagellate
623 *Micromonas pusilla*. *Nature* **281**: 299-301.
- 624 McDaniel L, Houchin LA, Williamson SJ, Paul JH. (2002). Lysogeny in marine
625 *Synechococcus*. *Nature* **415**: 496-496.
- 626 McDaniel LD, delaRosa M, Paul JH. (2006). Temperate and lytic cyanophages from
627 the Gulf of Mexico. *Journal of the Marine Biological Association of the United*
628 *Kingdom* **86**: 517-527.
- 629 Mojica KDA, Brussaard CPD. (2014). Factors affecting virus dynamics and microbial

- 630 host -virus interactions in marine environments. *FEMS Microbiology Ecology* **89**:
631 495-515.
- 632 Mojica KDA, Huisman J, Wilhelm SW, Brussaard CPD. (2015). Latitudinal variation
633 in virus-induced mortality of phytoplankton across the North Atlantic Ocean. *The*
634 *ISME Journal* **10**: 500-513.
- 635 Monier A, Comte J, Babin M, Forest A, Matsuoka A, Lovejoy C. (2015).
636 Oceanographic structure drives the assembly processes of microbial eukaryotic
637 communities. *The ISME Journal* **9**: 990–1002.
- 638 Nagasaki K, Yamaguchi M. (1998). Effect of temperature on the algicidal activity and
639 the stability of HaV (Heterosigma akashiwo virus). *Aquatic Microbial Ecology* **15**:
640 211-216.
- 641 Not F, Latasa M, Marie D, Cariou T, Vaultot D, Simon N. (2004). A Single Species,
642 *Micromonas pusilla* (Prasinophyceae), Dominates the Eukaryotic Picoplankton in the
643 Western English Channel. *Applied and Environmental Microbiology* **70**: 4064–4072.
- 644 Peperzak L, Brussaard C. (2011). Flow cytometric applicability of fluorescent vitality
645 probes on phytoplankton. *Journal of Phycology* **47**: 692-702.
- 646 Ras M, Steyer J-P, Bernard O. (2013). Temperature effect on microalgae: a crucial
647 factor for outdoor production. *Review Environmental Science Biotechnology* **12**: 153-
648 164.
- 649 Raven JA, Geider RJ. (1988). Temperature and algal growth. *New Phytologist* **110**:
650 441-461.
- 651 Sahlsten E. (1998). Seasonal abundance in Skagerrak-Kattegat coastal waters and host
652 specificity of viruses infecting the marine photosynthetic flagellate *Micromonas*
653 *pusilla*. *Aquatic Microbial Ecology* **20**: 2207-2212.
- 654 Šlapeta J, López-García P, Moreira D. (2006). Global dispersal and ancient cryptic
655 species in the smallest marine eukaryotes. *Molecular Biology and Evolution* **23**: 23–
656 29.
- 657 Suttle CA. (2005). Viruses in the sea. *Nature* **437**: 356-361.
- 658 Suttle CA. (2007). Marine viruses - major players in the global ecosystem. *Nature*
659 *Reviews Microbiology* **5**: 801-812.
- 660 Taylor J. (1962). The estimation of numbers of bacteria by tenfold dilution series.
661 *Journal of Applied Bacteriology* **25**: 54-61.
- 662 Thomas R, Grimsley N, Escande M-L, Subirana L, Derelle E, Moreau H. (2011).
663 Acquisition and maintenance of resistance to viruses in eukaryotic phytoplankton
664 populations. *Environmental Microbiology* **13**: 1412-1420.
- 665 Thomas R, Jacquet S, Grimsley N, Moreau H. (2012). Strategies and mechanisms of
666 resistance to viruses in photosynthetic aquatic microorganisms. *Advances in*
667 *Oceanography and Limnology* **3**: 1-15.

- 668 Thomsen HA, Buck KR. (1998). Nanoflagellates of the central California waters:
669 taxonomy, biogeography and abundance of primitive, green flagellates
670 (Pedinophyceae, Prasinophyceae). *Deep Sea Research Part II: Tropical Studies in*
671 *Oceanography* **45**: 1-21.
- 672 Tomaru Y, Tanabe H, Yamanaka S. (2005). Effects of temperature and light on
673 stability of microalgal viruses, HaV, HcV and HcRNAV. *Plankton Biology and*
674 *Ecology* **52**: 1-6.
- 675 Tomaru Y, Kimura K, Yamaguchi H. (2014). Temperature alters algicidal activity of
676 DNA and RNA viruses infecting *Chaetoceros tenuissimus*. *Aquatic Microbial*
677 *Ecology* **73**: 171-183.
- 678 Toseland A, Daines SJ, Clark JR, Kirkham A, Strauss J, Uhlig C, *et al.* (2013). The
679 impact of temperature on marine phytoplankton resource allocation and metabolism.
680 *Nature Climate Change* **3**: 979-984.
- 681 Waters RE, Chan AT. (1982). Micromonas-Pusilla Virus - the Virus Growth-Cycle
682 and Associated Physiological Events Within the Host-Cells - Host Range Mutation.
683 *Journal of General Virology* **63**: 199-206.
- 684 Weinbauer MG, Suttle CA. (1999). Lysogeny and prophage induction in coastal and
685 offshore bacterial communities. *Aquatic Microbial Ecology* **18**: 217-225.
- 686 Weinbauer MG, Christaki U, Nedoma J, Simek K. (2003). Comparing the effects of
687 resource enrichment and grazing on viral production in a meso-eutrophic reservoir.
688 *Aquatic Microbial Ecology* **31**: 137-144.
- 689 Wilhelm SW, Suttle CA. (1999). Viruses and Nutrient Cycles in the Sea Viruses play
690 critical roles in the structure and function of aquatic food webs. *BioScience* **49**: 781-
691 788.
- 692 Williamson SJ, Houchin LA, McDaniel L, Paul JH. (2002). Seasonal variation in
693 lysogeny as depicted by prophage induction in Tampa Bay, Florida. *Applied and*
694 *Environmental Microbiology* **68**: 4307-4314.
- 695 Wilson WH, Mann NH. (1997). Lysogenic and lytic viral production in marine
696 microbial communities. *Aquatic Microbial Ecology* **13**: 95-100.
- 697 Wilson WH, Francis I, Ryan K, Davy S.K. (2001). Temperature induction of viruses
698 in symbiotic dinoflagellates. *Aquatic Microbial Ecology* **25**: 99-102.
- 699 Yau S, Grimsley N, Moreau H. (2015). Molecular ecology of Mamiellales and their
700 viruses in the marine environment. *Perspectives in Phycology* **2**: 83–89.
- 701 Zingone A, Sarno D, Forlani G. (1999). Seasonal dynamics in the abundance of
702 *Micromonas pusilla* (Prasinophyceae) and its viruses in the Gulf of Naples
703 (Mediterranean Sea). *Journal of Plankton Research* **21**: 2143–2159.
- 704 Zingone A, Natale F, Biffali E, Borra M, Forlani G, Sarno D. (2006). Diversity in
705 morphology, infectivity, molecular characteristics and induced host resistance
706 between two viruses infecting *Micromonas pusilla*. *Aquatic Microbial Ecology* **45**: 1–

707 14.

708

709

710

711 **Figure and table legends**

712

713 **Table 1:** *Micromonas* and virus strains used in this study. Mic-A, Mic-B, and Mic-C
714 strains belong to *Micromonas* clade A, B, and C, respectively.

715 **Table 2:** Cardinal temperatures ($^{\circ}\text{C}$), optimal growth rates (d^{-1}) and their respective
716 confidence intervals (CI_{low} and CI_{up}) for the three *Micromonas* strains.

717 **Figure 1:** Flow cytograms representing (A) *Micromonas* cells discriminated using the
718 red fluorescence and the side scatter channels for total cell enumeration, (B)
719 *Micromonas* membrane integrity upon SYTOX-Green staining which discriminates
720 dead cells and live cells based on the green fluorescence channel. (C) MicV particles
721 discriminated by their green fluorescence and side scatter channels upon staining with
722 the nucleic acid dye SYBR-Green.

723 **Figure 2:** Growth response to temperature of *Micromonas sp.* strains Mic-A (red),
724 Mic-B (green) and Mic-C (blue). Closed circles represent experimental data and solid
725 lines indicate the fit of the CTMI model from Bernard and Rémond (2012). Error bars
726 represent the standard deviation of the data (at 95%, at least $n = 3$).

727 **Figure 3:** Decay rates of viral particles (dashed line) and viral infectivity (solid line)
728 for MicV-A, MicV-B, and MicV-C exposed to a large range in temperatures over a
729 6-week incubation period. Error bars represent the confidence intervals (at 95%, $n =$
730 3).

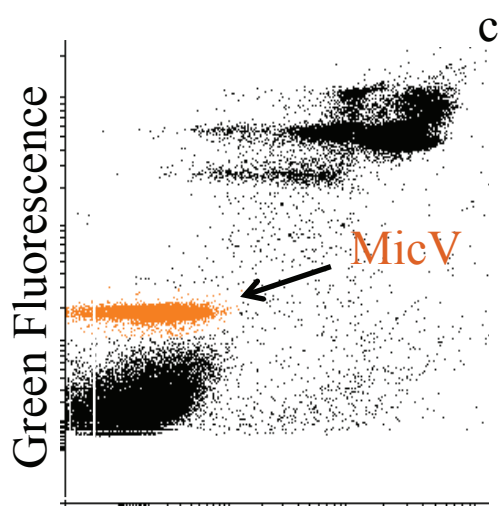
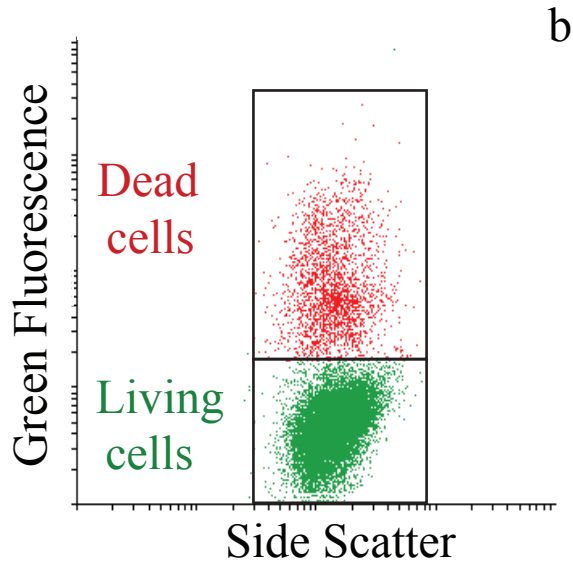
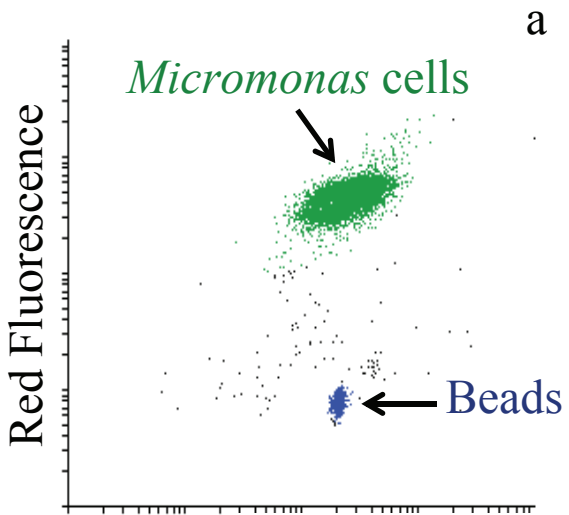
731 **Figure 4:** Viral infection of *Micromonas* Mic-B by MicV-B at 9.5, 12.5, 20, 25, 27.5,
732 and 30 $^{\circ}\text{C}$. Dynamics of viral abundance (panels a to f, data in grey triangles and

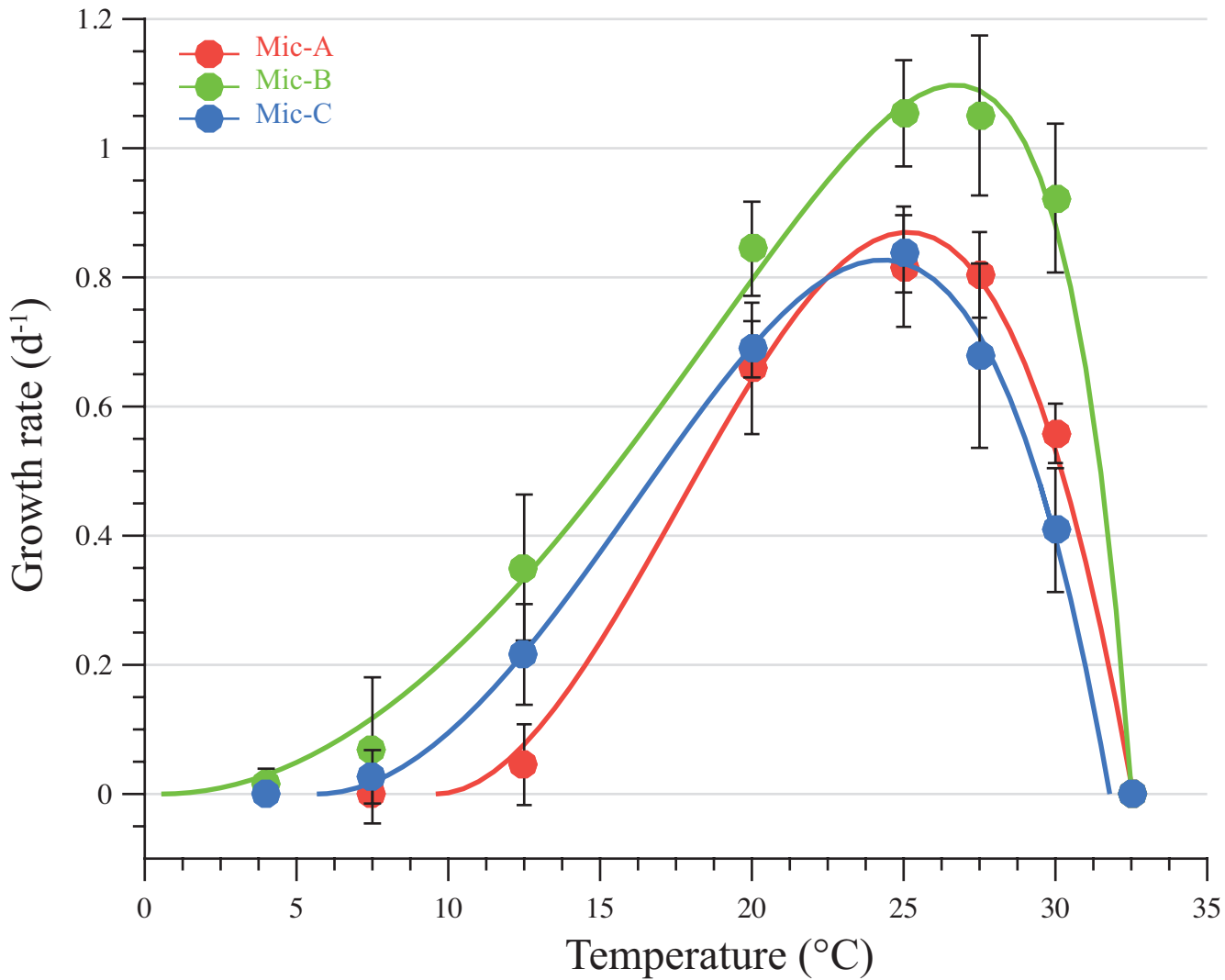
733 mean of two replicates in black lines), *Micromonas* abundance (panels g to l) in
734 control (dashed lines and white circles) and infected (solid lines and black circles)
735 cultures, % cells with intact membranes (viable cells, panels m to r) in control (dashed
736 lines and white circles) and infected (solid lines and black circles) cultures, and
737 photosynthetic capacity (panels s to y) of control (dashed lines and white circles) and
738 infected (solid lines and black circles) cultures are shown. Blues bars represent the
739 light phases. Error bars were computed from triplicate samples for the host
740 parameters. Virus particles were enumerated from duplicate samples, so no error bar
741 is shown.

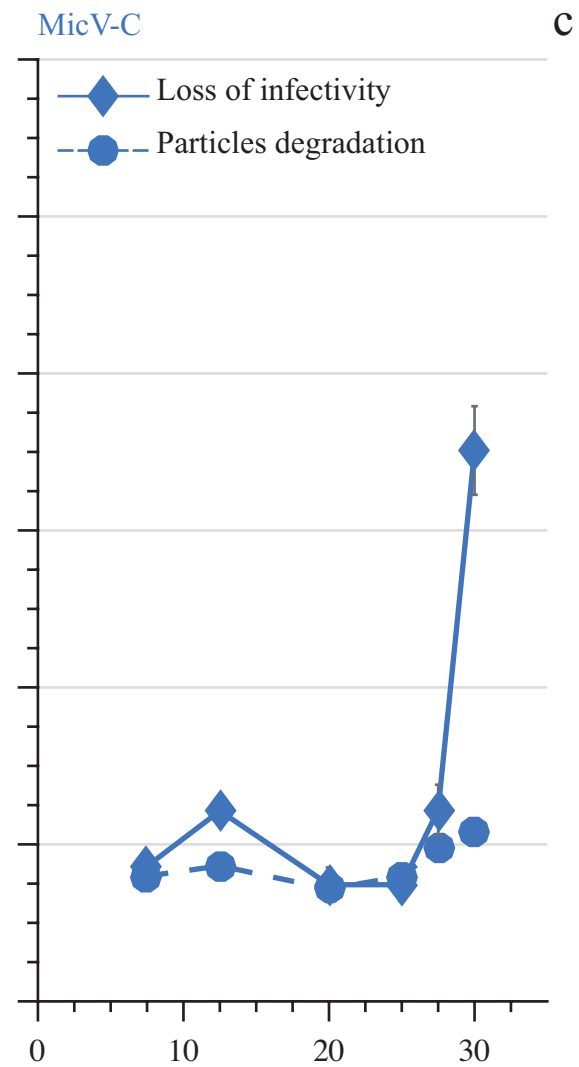
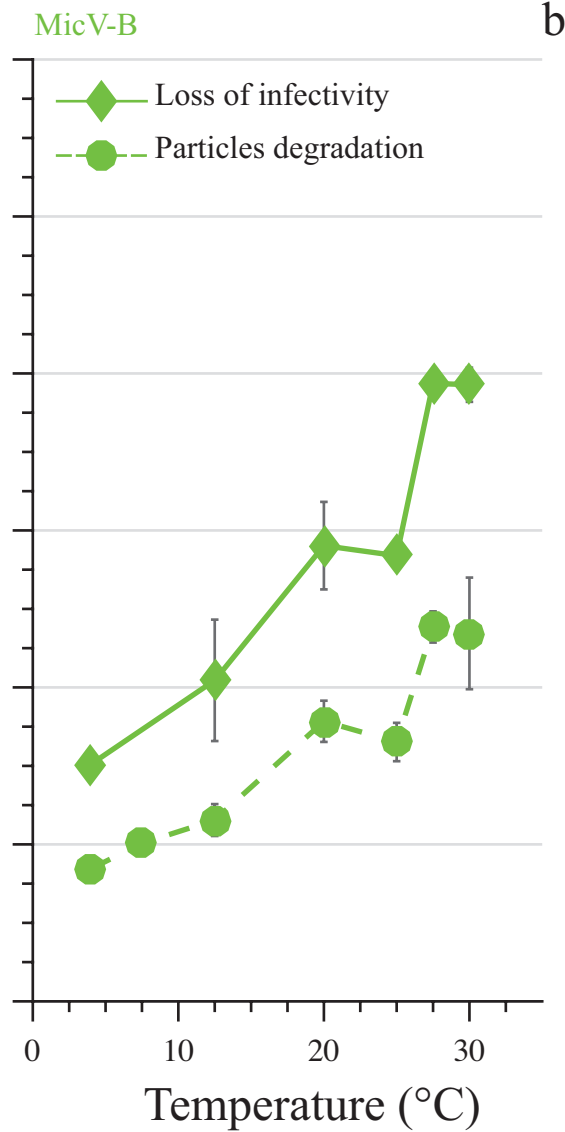
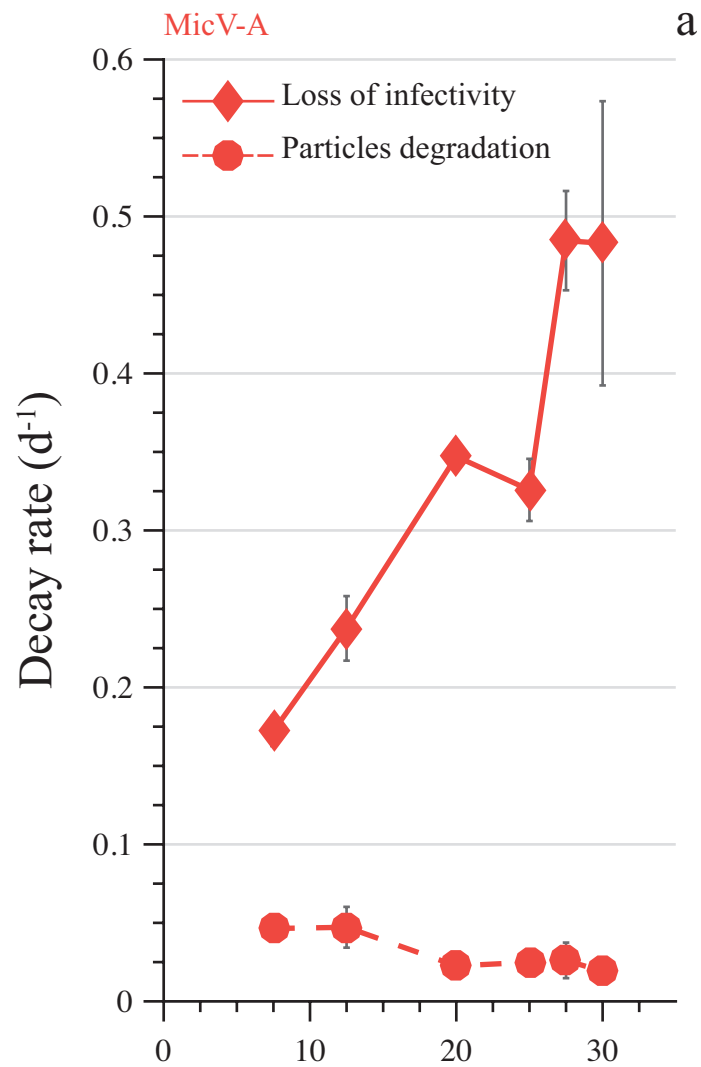
742 **Figure 5:** Relationship between viral latent period (dashed line and white circle), viral
743 production (solid line and black circle), and host growth rate for the system Mic-B /
744 MicV-B. Linear regressions were statistically robust with an adjusted $R^2 > 0.85$ and a
745 p -value < 0.05 .

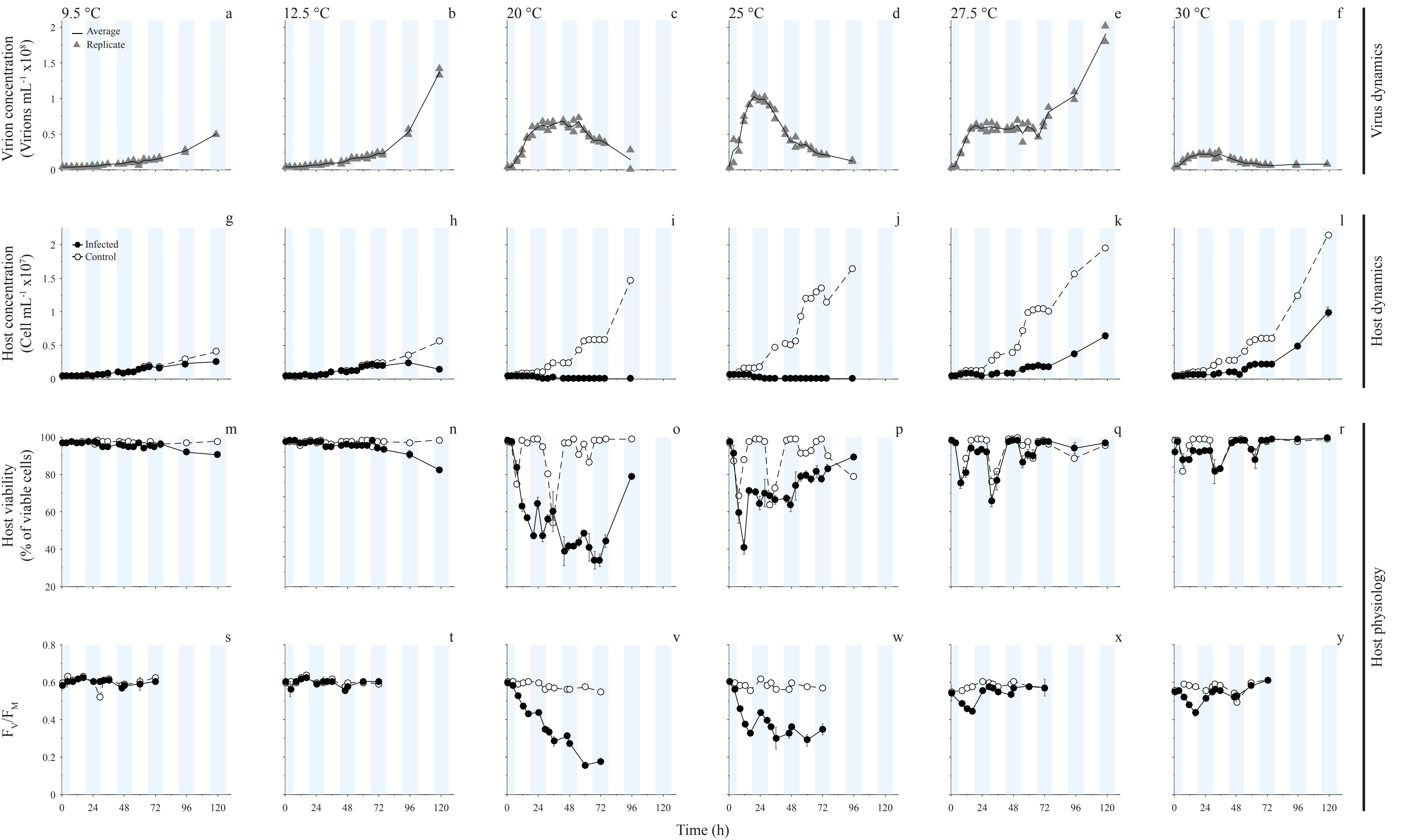
746 **Figure 6:** Viral infection of *Micromonas* Mic-A by MicV-A (black symbols and
747 lines) and *Micromonas* Mic-C by MicV-C (grey symbols and lines) at 12.5, 20, 27.5,
748 and 30 °C. Dynamics of virus abundance (a to e) for MicV-A (black triangles) and
749 MicV-C (grey triangles) are shown in the upper panels. Dynamics of *Micromonas*
750 abundance (e to i) for Mic-A in control (black open circles and dashed lines) and
751 infected cultures (black circles and solid lines) and Mic-C in control (grey open
752 circles and dashed lines) and infected cultures (grey circles and solid lines) are shown
753 in the bottom panels.

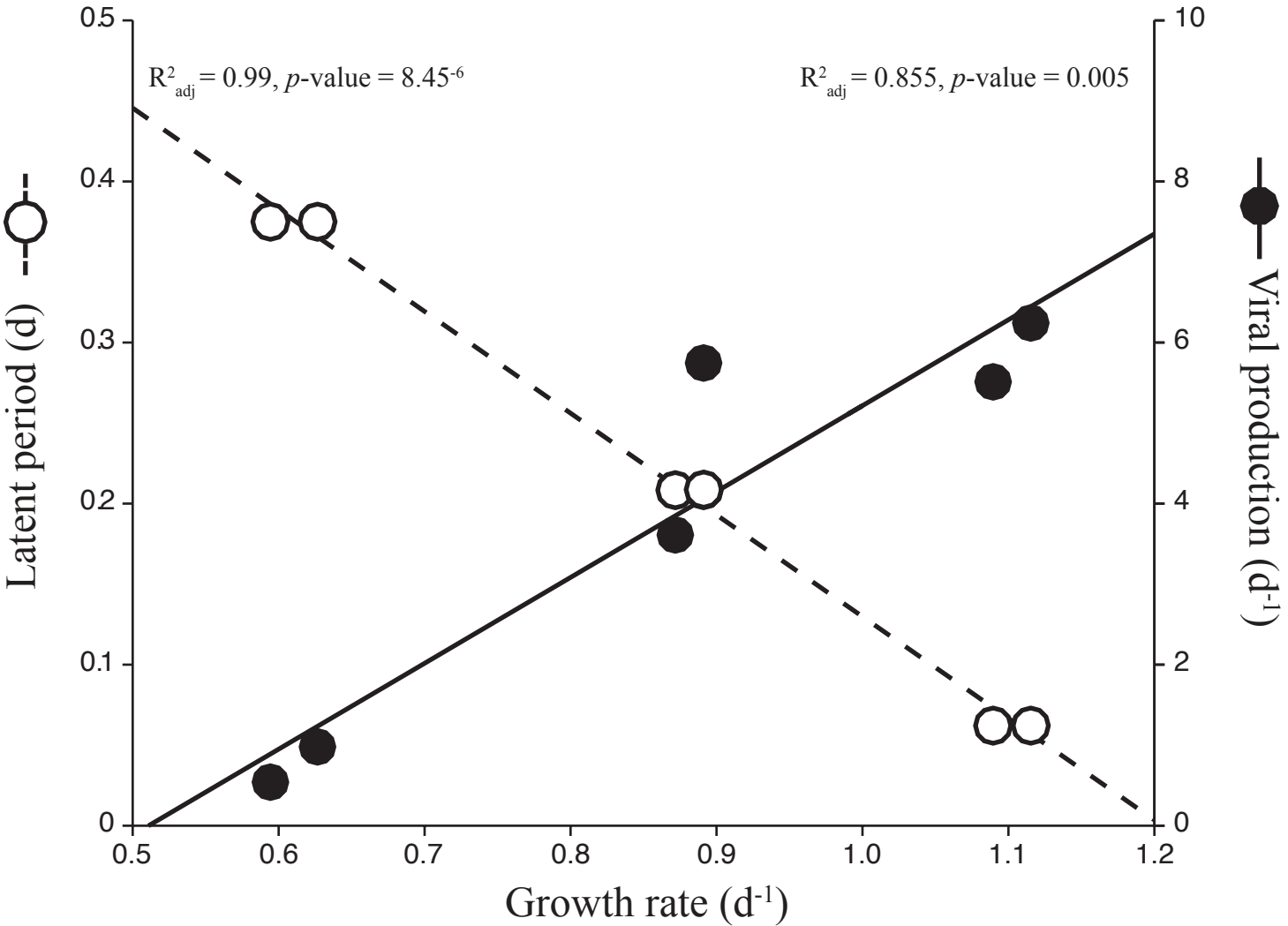
754

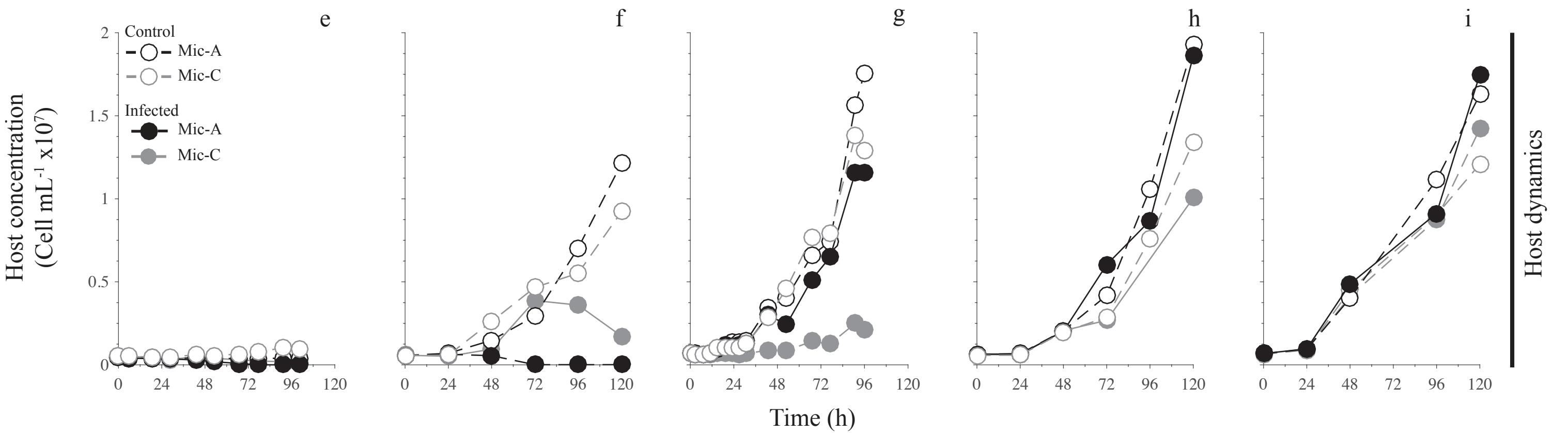
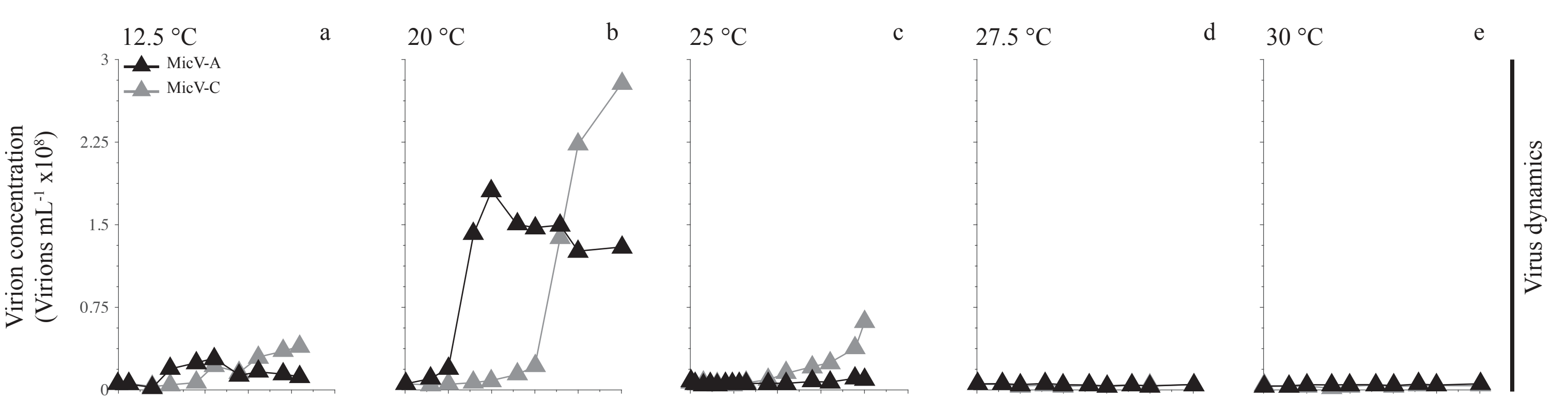












| Clade | <i>Micromonas</i> | | | Virus | | | | | |
|-------|-------------------|--------------|------------------------------|---------|--------------|------------------------------------|-------------------------|--|---|
| | RCC # | Strain name* | Isolation site and date | RCC # | Strain name* | Isolation site and date (mm/dd/yy) | Host range [§] | Latent period at 20°C (hours) [§] | <i>polB</i> accession number [§] |
| A | RCC451 | Mic-A | 72.2 W 38.4 N 07/11/80 | RCC4253 | MicV-A | 3.57 W 48.45 N 05/04/09 | Clade A | < 5 | KP734133 |
| B | RCC829 | Mic-B | 14.3 E 40.7 N 01/08/97 | RCC4265 | MicV-B | 3.57 W 48.45 N 09/28/09 | Clade A and B | 13 | KP734154 |
| C | RCC834 | Mic-C | 4.2 W 50.4 N 01/01/50 | RCC4229 | MicV-C | 3.57 W 48.45 N 03/02/09 | Clade C | 24-27 | KP734144 |

* These denominations are used only in this study

§ These informations are from Baudoux *et al.* 2015

| <i>Micromonas</i> strains | Mic-A | Mic-B | Mic-C |
|--|--------------------|----------------------|--------------------|
| $T_{\min} (CI_{\text{low}}-CI_{\text{up}})$ | 9.6 (7.5 - 11.5) | 0.55 (-2.3 - 3.3) | 5.7 (3.3 - 7.9) |
| $T_{\text{opt}} (CI_{\text{low}}-CI_{\text{up}})$ | 25.1 (24.5 - 25.8) | 26.7 (25.9 - 27.5) | 24.3 (23.4 - 25.2) |
| $T_{\max} (CI_{\text{low}}-CI_{\text{up}})$ | 32.6 (32.4 - 32.7) | 32.5 (32.49 - 32.53) | 31.8 (30.3 - 33.2) |
| $\mu_{\text{opt}} (CI_{\text{low}}- CI_{\text{up}})$ | 0.87 (0.82 - 0.92) | 1.1 (1.05 - 1.15) | 0.83 (0.76 - 0.87) |